Electronic Supplementary Material (ESI) for Green Chemistry.

Supporting information

Hydrothermally Stable Ru/HZSM-5 Catalyzed Selective Hydrogenolysis of Lignin-derived Substituted Phenols to Bio-Arenes in Water

Zhicheng Luo,[a] Zhaoxia Zheng,[a] Yuechao Wang,[b] Geng Sun,[b] Hong Jiang*[b], Chen Zhao*[ac]

[a] Shanghai Key Laboratory of Green Chemistry and Chemical Processes, School of Chemistry and Molecular Engineering, East China Normal University, Shanghai, 200062, China

E-mail: czhao@chem.ecnu.edu.cn (C. Zhao)

[b] Beijing National Laboratory for Molecular Sciences, State Key Laboratory of Rare Earth Materials Chemistry and Applications, College of Chemistry and Molecular Engineering, Peking University, Beijing 100871, China.

E-mail: h.jiang@pku.edu.cn (H. Jiang)

[c]Key Laboratory of Low-Carbon Conversion Science & Engineering, Shanghai Advanced Research Institute, Chinese Academy of Sciences, 201210, Shanghai, China

Experimental Section

Chemicals

$RuCl_3 \cdot 3H_2O$ (J&K, ≥ 59.5 wt%), Al_2O_3 (J&K), ZrO_2 (J&K), Activated Clay (J&K), TiO_2 (J&K), SiO_2 (Micxy Reagent, 10-20 nm), tetra-propylammonium hydroxide (TPAOH, Sinopec Co., Ltd., 25 wt%), tetra-ethylorthosilicate (TEOS, Sinopec Co., Ltd., containing 28.4 wt% SiO_2). guaiacol (Sinopharm, > 98% GC assay), anisole (Sinopharm, CP), phenol (Sinopharm, AR), aluminium isopropoxide (AIP) (Sinopharm, CP), catechol (Sinopharm, AR), 4-methylguaiacol (J&K, > 99% GC assay), 4-ethylguaiacol (TCI, > 97% GC assay), 2,6-dimethoxyphenol ((J&K, > 98% GC assay), 2,6-dimethoxy-4-methyl-phenol (Alfa Aesar, > 97% GC assay), eugenol (J&K, > 98% GC assay), CH_2Cl_2 (Sinopharm, AR), ethyl acetate (Sinopharm, AR). Air, H_2, and N_2 gases (99.999 vol.%) were supplied by Shanghai Pujiang Specialty Gases Co., Ltd.

Synthesis of HZSM-5

For HZSM-5 (SiO_2/Al_2O_3: 100) synthesis, AIP (2.4778 g) was dissolved in a mixture of TPAOH (122.016 g) and distilled water (70.488 g) with stirring at ambient temperature for 2 h until AIP was totally dissolved. Then TEOS (126.762 g) was added drop-wise into the mixed solution and kept stirring for 4 h, leading to a gel in which chemical composition was 1 SiO_2: 100 Al_2O_3: 15 H_2O : 0.25 TPAOH, before being transferred into a Teflon-lined stainless steel autoclave. Crystallization in an oven lasted for 72 h at 170 °C. After cooled down to ambient temperature naturally, the solid product was washed to neutrality, and sequentially centrifugated to remove supernatant liquid, and finally collected after drying at 110 °C overnight. Prior to use, it was calcined in flowing air (flowing rate: 100 $mL \cdot min^{-1}$) at 550 °C for 6 h.

Computational Details

The calculations of the dissociation energies at different positions were undertaken by using the B3LYP [1] density functional theory (DFT) with the 6-311G(d,p) basis set as implemented in Gaussian 09 [2].

Theoretical study of the dissociation of the guaiacol molecule on the Ru surface is based on a slab model of four atomic layers with a 4x4 supercell of Ru(0001) surface. All surface calculations are carried out by using density functional theory with the Perdew-Burke-Ernzerhof (PBE) generalized gradient approximation to the

exchange-correlation energy [3], the projector augmented wave (PAW) approach to core-valence interactions, and the plane wave basis, as implemented in the VASP package [4]. The energy cutoff for plane waves are 400 eV, the Brillouin zone is sampled with a 3x3x1 k-mesh. During the structure optimization, the two atomic layers of Ru in the bottom are fixed and the structures are considered to be fully optimized when the maximum force on each atom is less than 0.03 eV/Ang. The reaction barrier is determined by using the climb-image nudged elastic band (CI-NEB) approach [5].

Table S1. Acid sites characterization of Ru based catalysts by IR spectroscopy of adsorbed pyridine (Py-IR).

Catalyst	Acid Sites (Py-IR, mmol·g^{-1})		
	BAS	LAS	Total
Ru/Al_2O_3	0	0.042	0.042
Ru/ZrO_2	0	0.05	0.05
Ru/TiO_2	0	0	0
Ru/Activated Clay	0	0.071	0.071
Ru/SiO_2	0	0	0
Ru/HZSM-5(100)	0.175	0.075	0.25

Table S2. Hydrogenolysis of guaiacol with different supported metallic catalysts in the gas phase.

Catalyst	Reaction Condition			Gas composition	Major products	Arene Yield (%)	Rate (g·g^{-1}·h^{-1})	Ref
	T (ºC)	P (MPa)	1/WHSV (h)					
Pt-Sn/CNF	400	0.1	3.2	0.6% GUA; 82.5% N_2; 16.9% H_2	Benzene, phenol, cresol, toluene, methane,	60	0.0115	[6]
Fe/SiO_2	400	0.1	1.5	1% GUA; 9% Ar; 90% H_2	Benzene, phenol, anisole, cresol, toluene, CH_4	38	0.057	[7]
PdFe/C	450	0.04	0.15	1% GUA, 99% H_2	Benzene/toluene/TMB	83	0.0012	[8]
Mo/C	380	4	0.067	4.8% GUA, 95.2% H_2	Benzene, phenol	84	0.0027	[9]
Ni_2P/SiO_2	300	0.1	2.0	0.024% GUA; 80% H_2,	Benzene, phenol, anisole	60	0.00029	[10]

Table S3. Physicochemical properties and acid sites characterization of the Ru/HZSM-5(100) sample.

Catalyst	Si/Al molar ratio [a]	S_{BET} ($m^2 \cdot g^{-1}$) [b]	V_{Pore} ($cm^3 \cdot g^{-1}$) [b]	Acid *conc.* ($mmol \cdot g^{-1}$) [c]
Ru/HZSM-5	100	424	0.34	0.210

[a] analyzed by ICP

[b] determined by N_2 sorption

[c] detected by TPD of absorbed NH_3

Table S4. Products distributions from guaiacol hydrodeoxygenation over supported Ru catalysts with different types of acid sites and pore structures in the aqueous phase.

Catalyst	Conv.	Yield (C%)					
		Meth-anol	Ben-zene	Cyclo-hexanol	Cyclo-hexanone	Phen-ol	2-Methoxy-Cyclohexanol
Ru/HZSM-5 (100)	100	4.0	96				
Ru/TS-1	100	3.3	76	3.1	3.6	14	
Ru/Silicalite-1	100	4.2	49	7.3	13	26	
Ru/SiO_2	100	2.5	50	18	4.1		25

General condition: guaiacol (0.2 g), Ru based catalysts (5 wt%, 0.20 g), H_2O (100 mL), 240 °C, 2 bar H_2 and 6 bar N_2, 1 h, stirring at 650 rpm.

Table S5. Products distribution from hydrodeoxygenation of cyclohexanol and cyclohexanone with Ru/HZSM-5 in aqueous phase.

Reactant	Conv.	Yield (C%)			
		Benzene	Cyclohexane	Cyclohexene	Cyclohexanol
Cyclohexanol	97	52	44	0.6	-
Cyclohexanone	100	35	62	0.8	2.2

General condition: reactant (1.0 g), Ru/HZSM-5 (5 wt%, 0.1 g), H_2O (100 mL), 240 °C, 2 bar H_2 and 6 bar N_2, 1 h, stirring at 650 rpm.

Table S6. The surface and pore properties of used Ru/HZSM-5(100) during four catalytic runs.

Ru/HZSM-5(100)	S_{meso} ($m^2 \cdot g^{-1}$)	S_{micro} ($m^2 \cdot g^{-1}$)	S_{BET} ($m^2 \cdot g^{-1}$)	V_{meso} ($cm^3 \cdot g^{-1}$)	V_{micro} ($cm^3 \cdot g^{-1}$)	V_{total} ($cm^3 \cdot g^{-1}$)
After Run 1	36	344	380	0.262	0.159	0.421
After Run 2	37	325	362	0.263	0.152	0.415
After Run 3	40	314	354	0.282	0.147	0.429
After Run 4	41	316	357	0.255	0.146	0.401

Table S7. DFT theoretical calculation results of two reaction pathways (at b and c positions as illustrated in Fig. 4) on the Ru (0001) surface.

Path	Reactant state	Transition state	Product state	E_a (eV)	ΔE_r (eV)
a	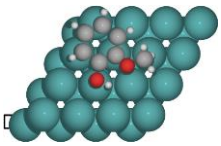	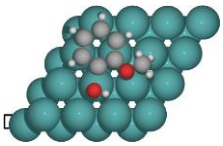	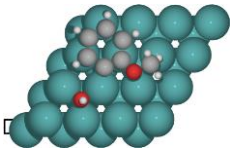	1.05	-0.03
b	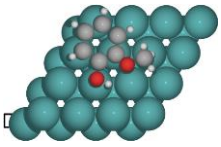	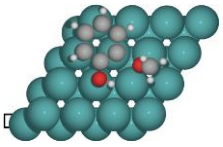	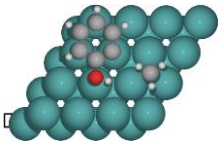	1.31	0.42
c	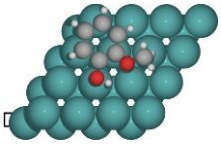	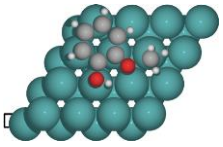	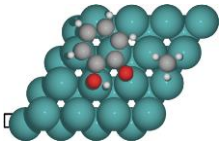	1.12	-0.65

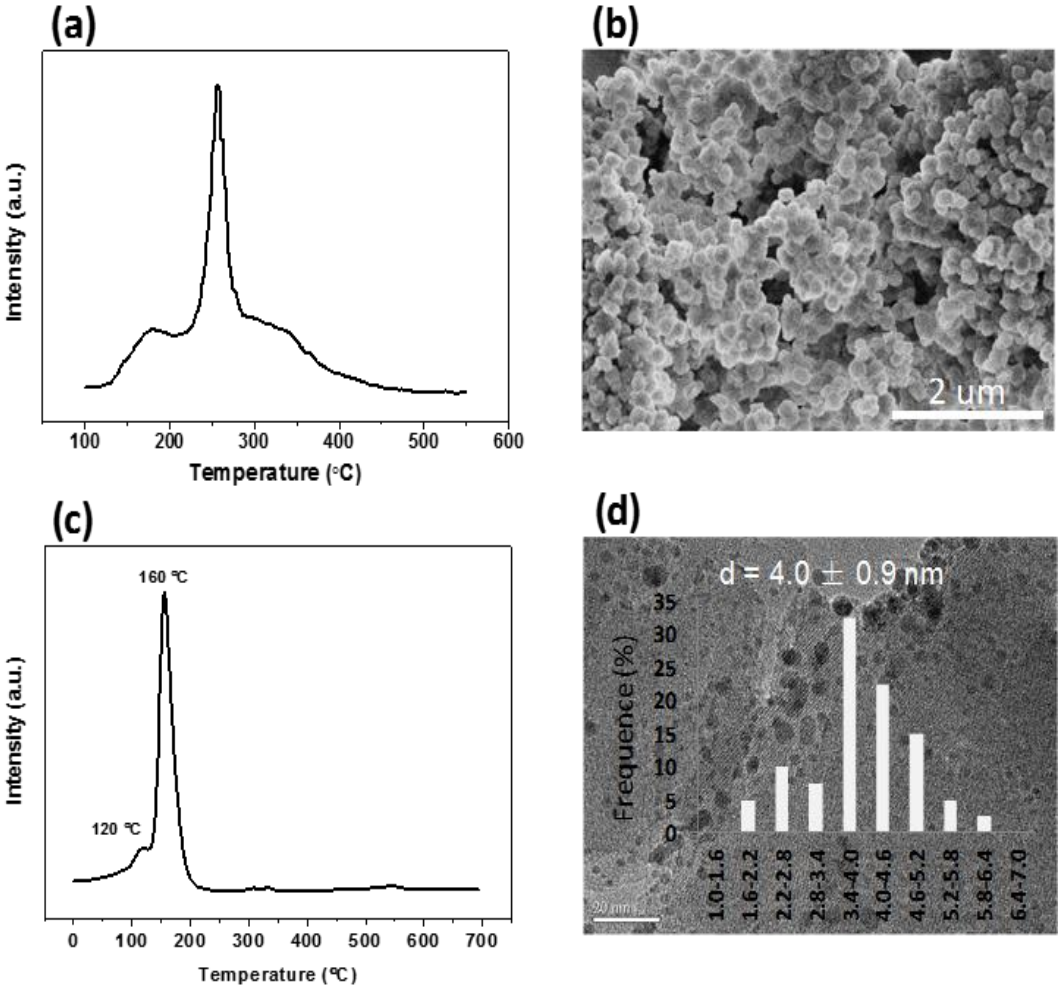

Figure S1. Characterization of Ru/HZSM-5 catalysts by (a) temperature programmed desorption of NH_3 measurement, (b) SEM image, (c) temperature programmed reduction of H_2, and (d) TEM image and particle size distribution.

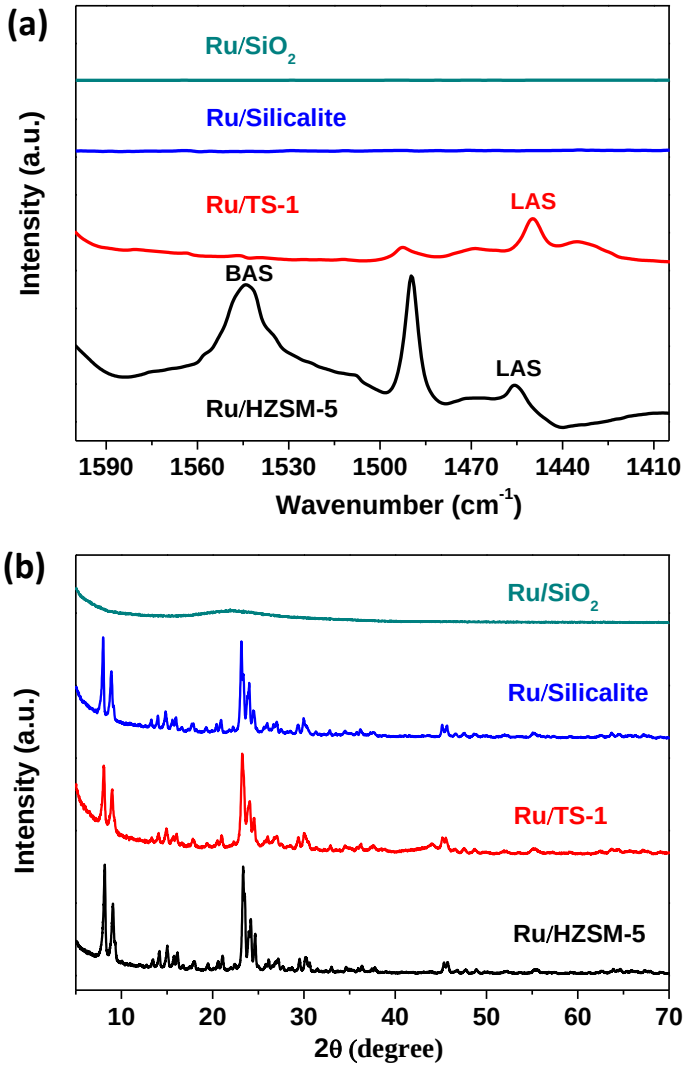

Figure S2. (a) IR spectra of adsorbed pyridine and (b) XRD patterns of diverse supported Ru catalysts.

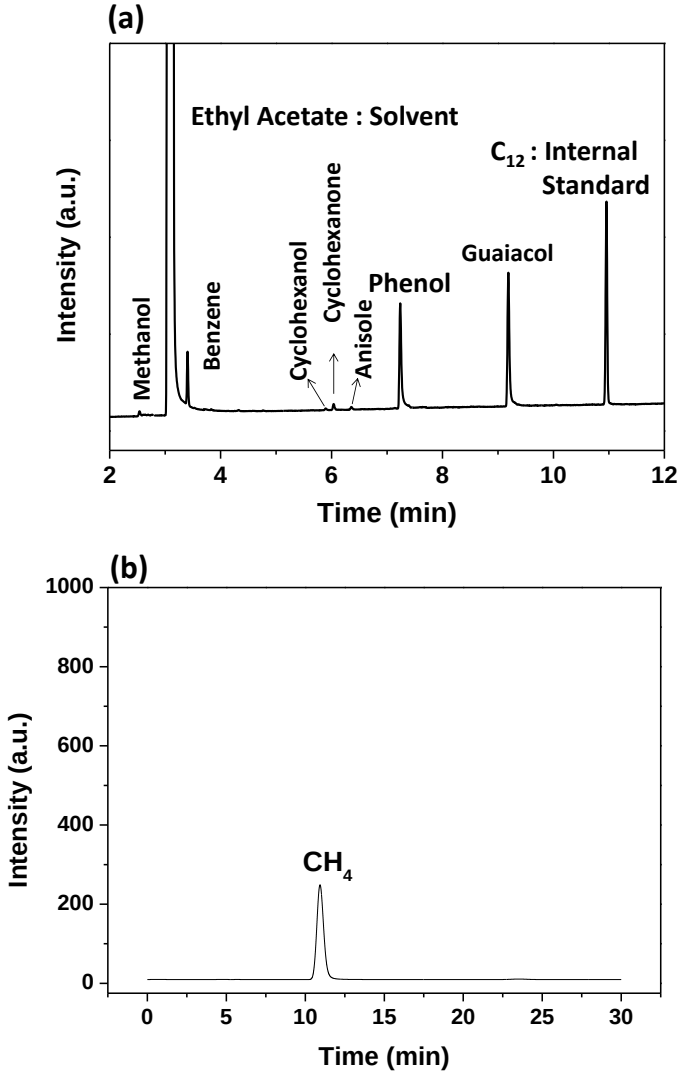

Figure S3. Characterization of the fresh and used Ru/HZSM-5 catalysts by (a) GC spectrum of organic-phase liquid products, (b) GC spectrum of gas-phase products.

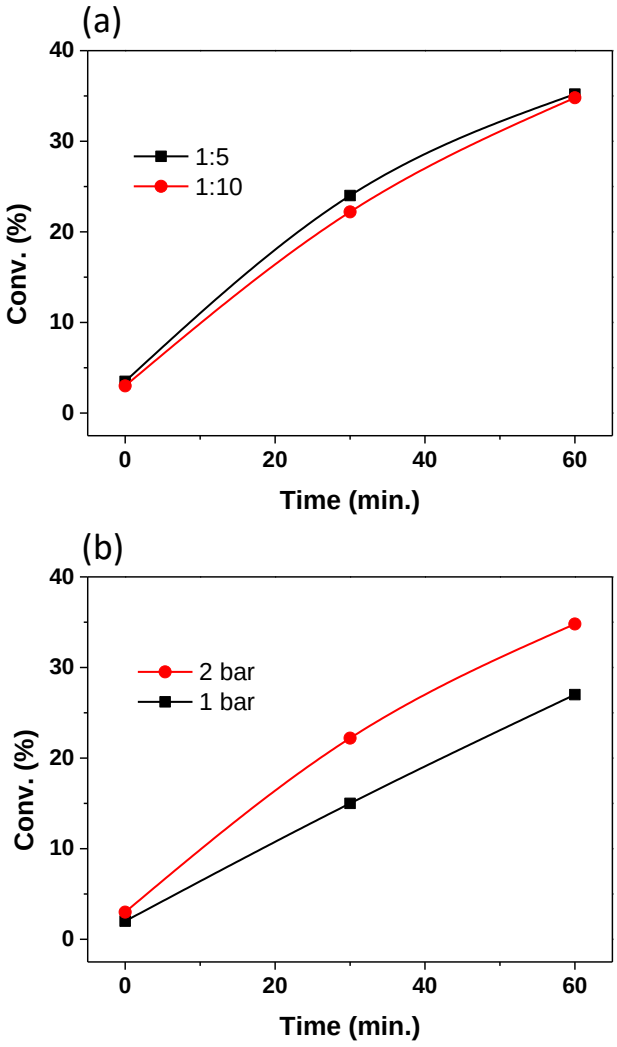

Figure S4. Kinetics of guaiacol conversion with varying (a) reactant to catalyst weight ratio (with 0.5 g or 1.0 g guaiacol), and (b) hydrogen pressures (1 and 2 bar) with 1.0 g guaiacol. General conditions: H_2O (100 mL), catalyst (0.1 g), 240 ˚C, stirring at 650 rpm.

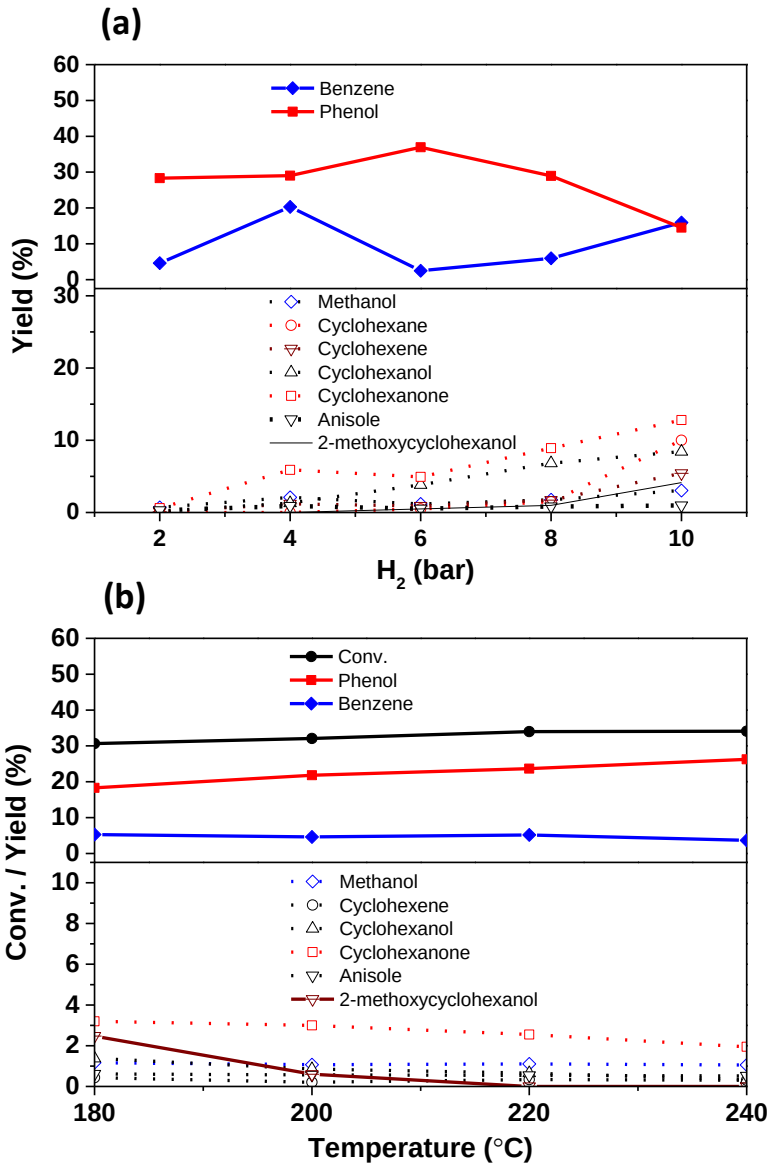

Figure S5. Influence of (a) hydrogen pressures and (b) temperatures towards product distributions of guaiacol conversion. Reaction conditions: guaiacol (1.0 g), Ru/HZSM-5 (5 wt%, 0.10 g), H_2O (100 mL), 1 h, stirring at 650 rpm.

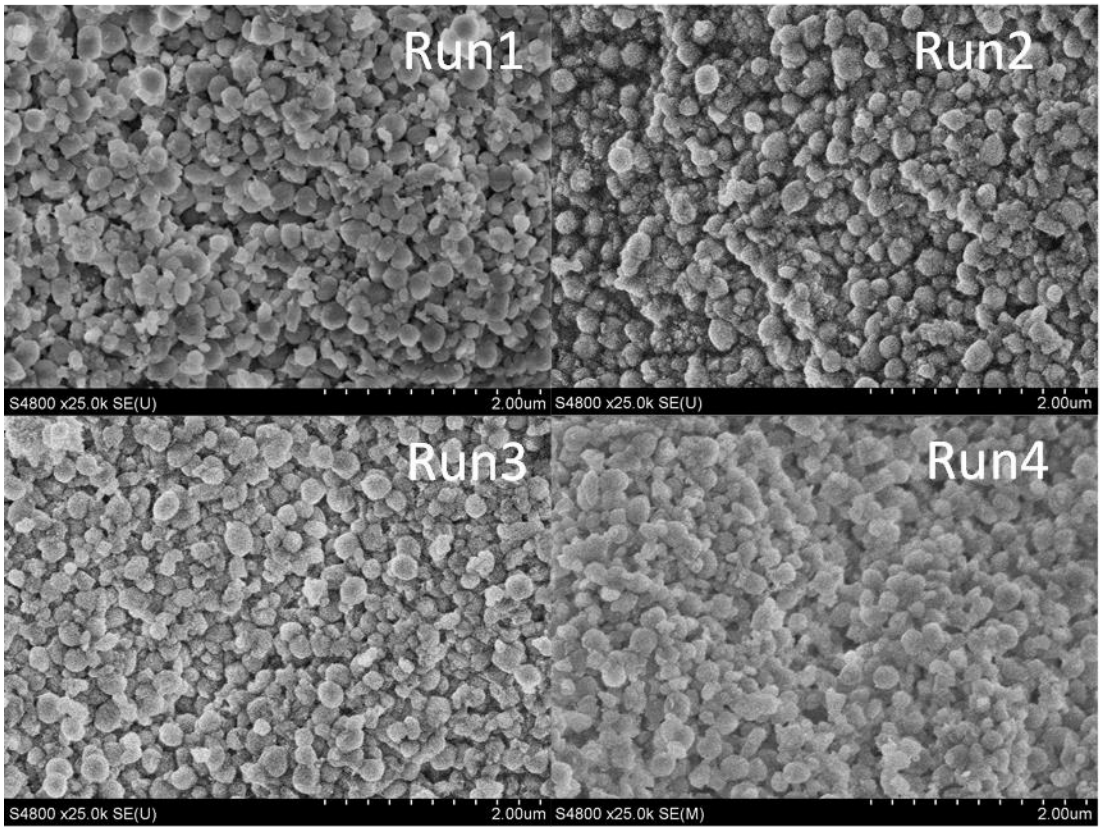

Figure S6. SEM images of used Ru/HZSM-5 after four catalytic runs.

References:

1. (a) Becke, A. D. J. Chem. Phys. **1993**, *98*, 5648-5652; (b) Lee, C.; Yang, W.; Parr, R. G. Phys. Rev. B, **1988**, *37*, 785-789.
2. Frisch, M. J.; Trucks, G. W.; Schlegel, H. B.; Scuseria, G. E.; Robb, M. A.; Cheeseman, J. R.; Scalmani, G.; Barone, V.; Mennucci, B.; Petersson, G. A.; Nakatsuji, H.; Caricato, M.; Li, X.; Hratchian, H. P.; Izmaylov, A. F.; Bloino, J.; Zheng, G.; Sonnenberg, J. L.; Hada, M.; Ehara, M.; Toyota, K.; Fukuda, R.; Hasegawa, J.; Ishida, M.; Nakajima, T.; Honda, Y.; Kitao, O.; Nakai, H.; Vreven, T.; Montgomery, J. A.; Peralta, J. E.; Ogliaro, F.; Bearpark, M.; Heyd, J. J.; Brothers, E.; Kudin, K. N.; Staroverov, V. N.; Kobayashi, R.; Normand, J.; Raghavachari, K.; Rendell, A.; Burant, J. C.; Iyengar, S. S.; Tomasi, J.; Cossi, M.; Rega, N.; Millam, J. M.; Klene, M.; Knox, J. E.; Cross, J. B.; Bakken, V.; Adamo, C.; Jaramillo, J.; Gomperts, R.; Stratmann, R. E.; Yazyev, O.; Austin, A. J.; Cammi, R.; Pomelli, C.; Ochterski, J. W.; Martin, R. L.; Morokuma, K.; Zakrzewski, V. G.; Voth, G. A.; Salvador, P.; Dannenberg, J. J.; Dapprich, S.; Daniels, A. D.; Farkas, O.; Foresman, J. B.; Ortiz, J. V.; Cioslowski, J.; Fox, D. J. Gaussian 09, revision A.02; Gaussian, Inc.: Wallingford, CT, **2009**.
3. Perdew, J. P., Burke, K. and Ernzerhof, M. Phys. Rev. Lett. **1996**, *77*, 3865-3868.
4. Kresse, G.; Furthmuller, J.; Comput. Mater. Sci. **1996**, *6*, 15-50.
5. Henkelman, G.; Uberuaga, B. P.; Jónsson, H. J. Chem. Phys. **2000**, *113*, 9901-9904.
6. Gonzalez-Borja, M. A.; Resasco, D. E. *Energy Fuels*, **2011**, *25*, 4155–4162.
7. Olcese, R. N.; Bettahar, M.; Petitjean, D.; Malaman, B.; Giovanella, F.; Dufour, A. *Appl. Catal. B,* **2012**, *115*, 63-73.
8. Sun, J.; Karim, A. M.; Zhang, H.; Kovarik, L.; Li, X. S.; Hensley, A. J.; Mcewen, J. S.; Wang, Y. *J. Catal.*, **2013**, *306*, 47-57.
9. Chang, J.; Danuthai, T.; Dewiyanti, S.; Wang, C.; Borgna, A. *ChemCatChem*, **2013**, *5*, 3041-3049.
10. Moon, J. S.; Kim, E. G.; Lee, Y. K. *J. Catal.*, **2014**, *311*, 144-152.